APPENDIX

Attenuation Compensation

Girard *et al.* developed an attenuation compensation algorithm to remove the OCT vessel shadows and enhance the contrast of optic nerve head.[A1] This algorithm was then employed in the calculation of the attenuation coefficients of retinal tissue,[A2] enhancing the visibility of lamina cribrosa,[A3] and improving the contrast of the choroid vasculature and the visibility of the sclera-choroid interface.[A4, A5] It can be expressed as:

$$I_{AC}(x,y) = \frac{I(x,y)}{2\sum_{k=x}^{M} I(k,y)}, \quad (1)$$

where I_{AC} is the AC-enhanced image intensity and I is the original image intensity. (x, y) are the pixel coordinates of the B-scan images ($x \in [1,\ M],\ y \in [1, N-1]$). M and N are the row and column numbers.

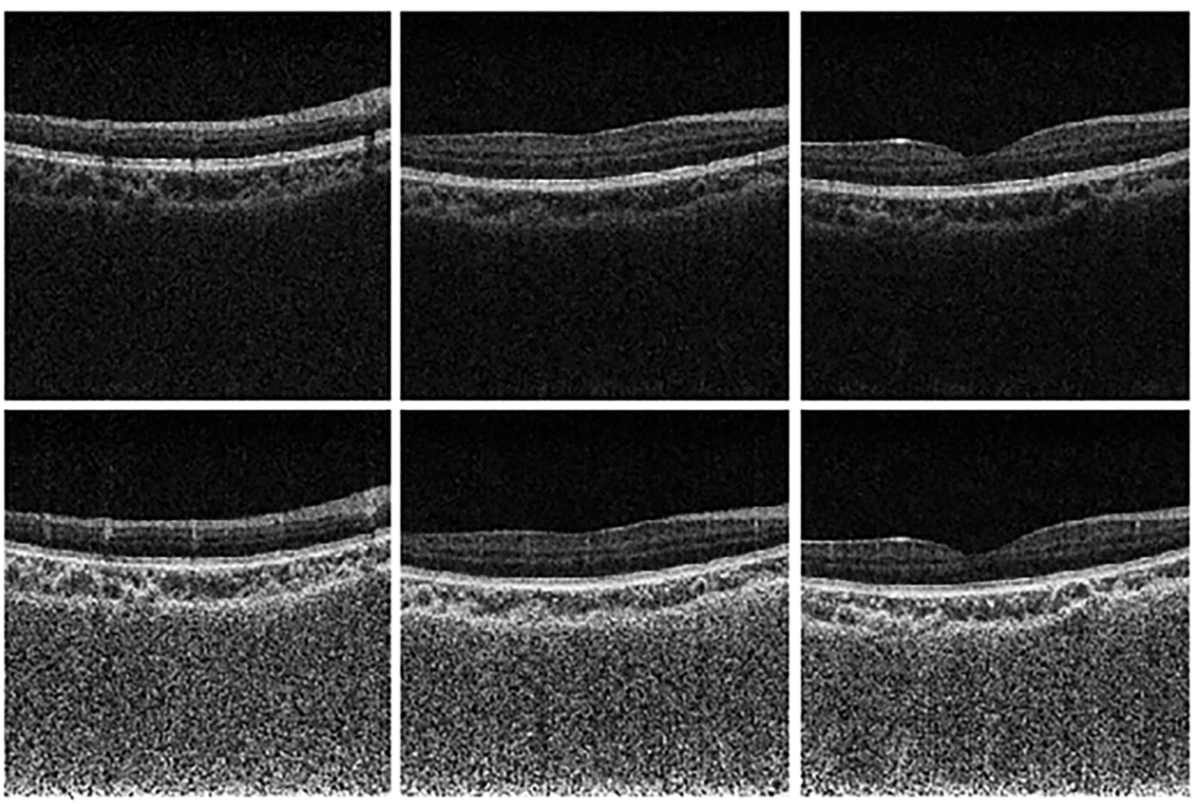

Figure A1. Examples of using attenuation compensation. Upper: Original B-scans. Lower: Enhanced B-scans.

Choroid Segmentation

We employ the U-shape convolutional network (U-Net)[A6] to automatically segment the choroid in OCT. As shown in Fig. A2, the U-Net a fully convolutional network that includes convolution (Conv 3×3 and Up conv 2×2), max pooling (Max pooling 2×2), and nonlinear activations (ReLU and Sigmoid). It uses an Encoder path (left) to extract features and a symmetric Decoder path (right) to precise localization. To get better precise locations, at every step of the decoder, the U-Net uses skip connections by concatenating the output of the transposed convolution layers with the feature maps from the Encoder at the same level. The U-Net has achieved tremendous success in various medical image and semantic segmentation tasks. It enables high segmentation accuracy with limited sample sizes.[A6, A7]

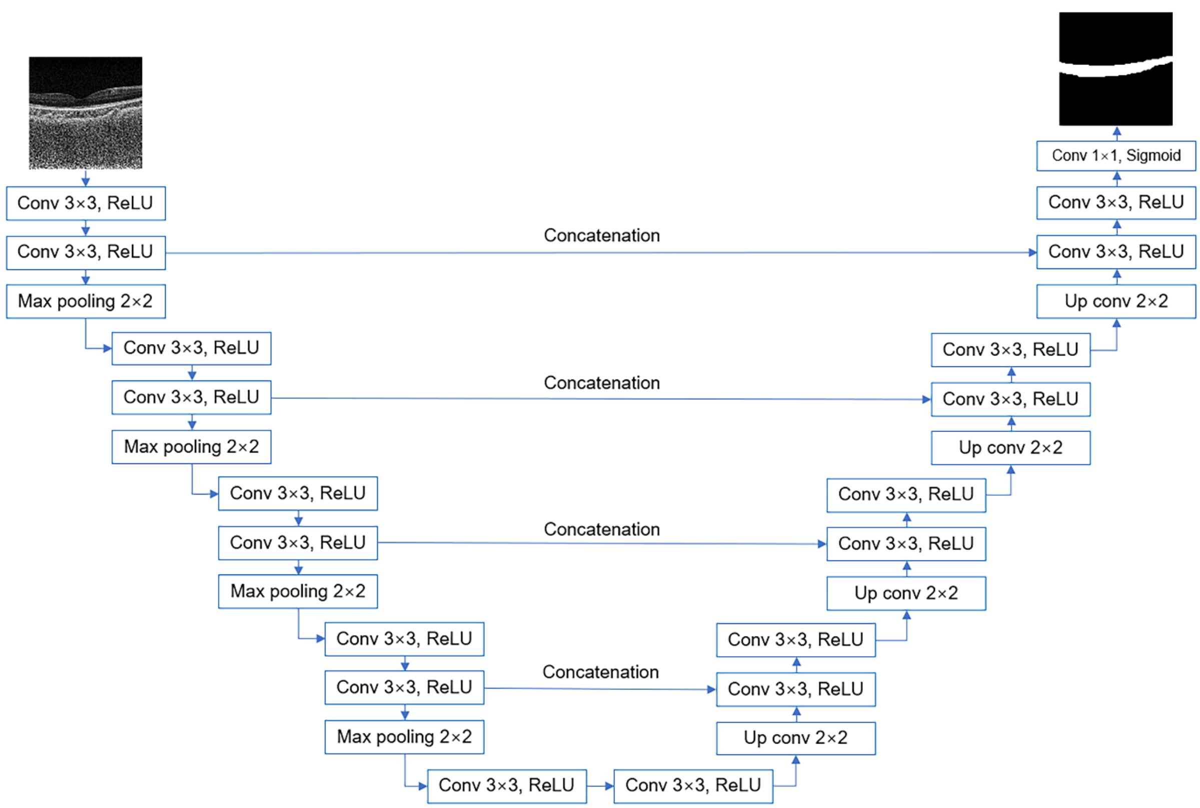

Figure A2. The U-shape convolutional neural network (U-Net) employed in the automatic segmentation of the choroid.

The U-Net for the choroid segmentation is implemented in Pytorch. We train the deep network with a total of 145 manually-annotated OCT B-scans. The training, validation, and testing sets are split with a ratio of 18:6:5. We employ the Adam optimizer with an initial learning rate of 10^{-5}. We train a total of 200 epochs for the convergence of the model. We employ the average unsigned surface detection error (AUSDE) to quantitatively evaluate the segmentation performance, which calculates the pixel-wise mismatch between the segmented choroid boundary and the manual ground truth. We achieve an AUSDE of 2.65 pixels using the test set. We then deploy the trained model to segment the data used in this paper. After the automatic segmentation, we manually check the results frame by frame. Figure A3 is the examples of segmented choroid using U-Net. Upper: Input B-scans. Lower: the corresponding segmentation results. We can see the automatic segmentation is accurate for different positions of the 6×6 mm^2 macular scans.

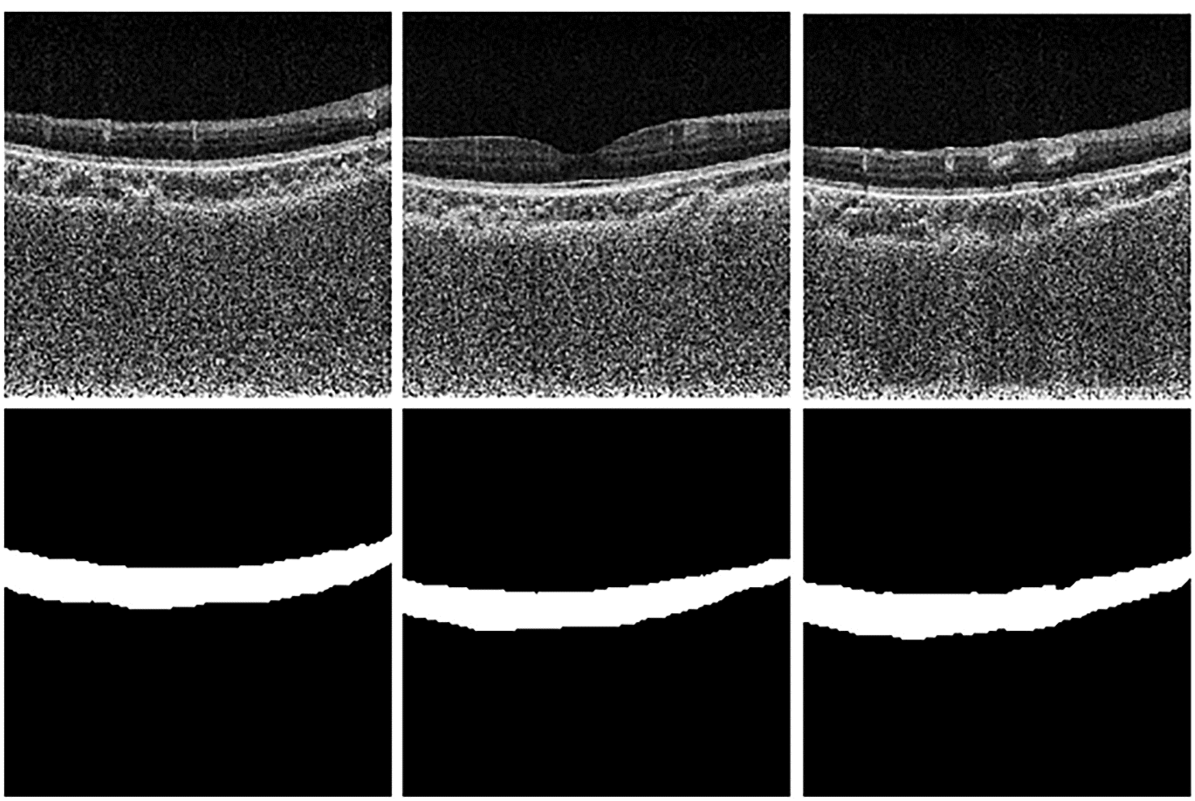

Figure A3 Examples of segmented choroid using U-Net. Upper: Input B-scans. Lower: the corresponding segmentation results.

En-face Mapping

To visualize the choroidal vasculature, we follow the *en face* mapping procedure in previous publications.[A8, A9] We project the content of the choroid region to *en face* plane using mean value mapping. Then we create the vessel density map by thresholding the *en face* choroidal vasculature with a level of one stand deviation lower than the mean value of a manually-selected vessel-free region. Figure A4 shows an example of choroidal vasculature. Right: Original *en face* mapping. Center: *en face* mapping after attenuation compensation. Right: Vessel density map. The vessel density can be calculated as[A10]:

$$vessel \;\; density = \frac{\int_A \; VdA}{\int_A \; dA}, \tag{2}$$

where A is the area used in the calculation. If the pixel belongs to a vessel, V=1, otherwise V=0.

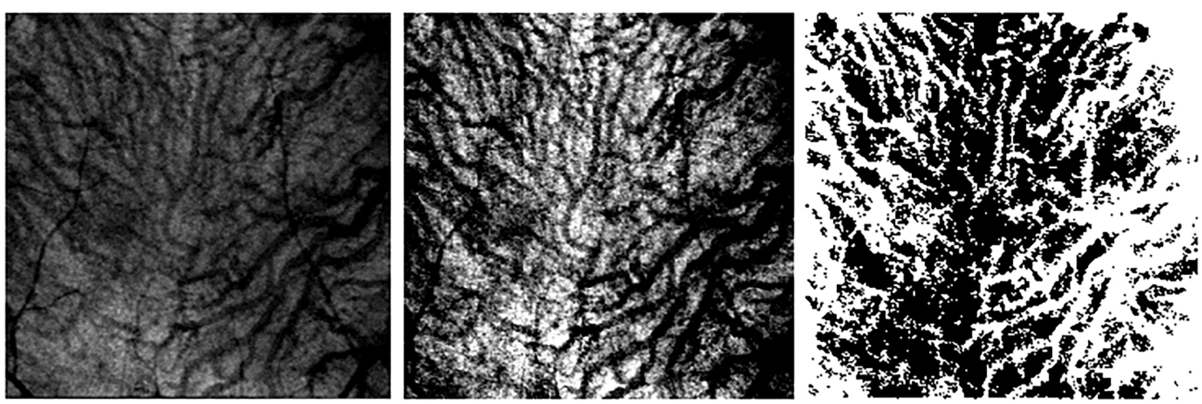

Figure A4. An example of choroidal vasculature. Right: Original *en face* mapping. Center: *en face* mapping after attenuation compensation. Right: Vessel density map.

REFERENCES

A1. Girard MJ, Strouthidis NG, Ethier CR, Mari JM. Shadow Removal and Contrast Enhancement in Optical Coherence Tomography Images of the Human Optic Nerve Head. Invest Ophthalmol Vis Sci 2011;52:7738-48.

A2. Vermeer K, Mo J, Weda J, et al. Depth Resolved Model-based Reconstruction of Attenuation Coefficients in Optical Coherence Tomography. Biomed Opt Express 2014;5:322-37.

A3. Mari JM, Strouthidis NG, Park SC, Girard MJ. Enhancement of Lamina Cribrosa Visibility in Optical Coherence Tomography Images Using Adaptive Compensation. Invest Ophthalmol Vis Sci 2013;54:2238-47.

A4. Zhou H, Chu Z, Zhang Q, et al. Attenuation Correction Assisted Automatic Segmentation for Assessing Choroidal Thickness and Vasculature with Swept-source OCT. Biomed Opt Express 2018;9:6067-80.

A5. Vupparaboina KK, Dansingani KK, Goud A, et al. Quantitative Shadow Compensated Optical Coherence Tomography of Choroidal Vasculature. Sci Rep 2018;8:6461.

A6. Ronneberger O, Fischer P, Brox T. U-net: Convolutional Networks for Biomedical Image Segmentation. International Conference on Medical Image Computing and Computer-assisted Intervention. Springer 2015:234-41.

A7. Ibtehaz N, Rahman MS. MultiResUNet: Rethinking the U-Net Architecture for Multimodal Biomedical Image Segmentation. Neural Netw 2020;121:74-87.

A8. Li F, Li H, Yang J, et al. Upsidedown Position Leads to Choroidal Expansion and Anterior Chamber Shallowing: OCT Study. Br J of Ophthalmol 2020;104:790-4.

A9. Yang J, Mu X, Zhao Y, et al. Enhancing Visibility of Choroidal Vasculature in OCT via Attenuation Compensation and Coherence Transport Inpainting. Invest Ophthalmol Vis Sci 2019;60:ARVO E-Abstract 148.

A10. Jia Y, Morrison JC, Tokayer J, et al. Quantitative OCT Angiography of Optic Nerve Head Blood Flow. Biomed Opt Express 2012;3:3127-37.